J|A|C|S COMMUNICATIONS

Published on Web 10/27/2010

Hydrogen-Storage Properties of Solid-Solution Alloys of Immiscible Neighboring Elements with Pd

Kohei Kusada,*[,†] Miho Yamauchi,[#] Hirokazu Kobayashi,[‡] Hiroshi Kitagawa,*[,†,‡,§] and Yoshiki Kubota[⊥]

Division of Chemistry, Graduate School of Science, Kyoto University, Kitashirakawa-Oiwakecho, Sakyo-ku, Kyoto 606-8502, Japan, Catalysis Research Center, Hokkaido University, Kita 21, Nishi 10, Kita-ku, Sapporo 001-0021, Japan, Institute for Integrated Cell-Material Sciences (iCeMS), Kyoto University, Yoshida, Sakyo-ku, Kyoto 606-8501, Japan, JST CREST, Sanbancho 5, Chiyoda-ku, Tokyo 102-0075, Japan, and Department of Physical Science, Graduate School of Science, Osaka Prefecture University, Sakai, Osaka 599-8531, Japan

Received August 16, 2010; E-mail: kusada@kuchem.kyoto-u.ac.jp; kitagawa@kuchem.kyoto-u.ac.jp

Abstract: Rh and Ag are the elements neighboring Pd, which is well known as a hydrogen-storage metal. Although Rh and Ag do not possess hydrogen-storage properties, can Ag−Rh alloys actually store hydrogen? Ag−Rh solid-solution alloys have not been explored in the past because they do not mix with each other at the atomic level, even in the liquid phase. We have used the chemical reduction method to obtain such Ag−Rh alloys, and XRD and STEM-EDX give clear evidence that the alloys mixed at the atomic level. From the measurements of hydrogen pressure−composition isotherms and solid-state ^{2}H NMR, we have revealed that Ag−Rh solid-solution alloys absorb hydrogen, and the total amount of hydrogen absorbed reached a maximum at the ratio of Ag:Rh = 50:50, where the electronic structure is expected to be similar to that of Pd.

Atomic-level (solid-solution) alloying has the advantage of allowing researchers to continuously control chemical and physical properties of elements by changing compositions and/or combinations of constituent elements.[1] However, solid-solution phases in alloys are limited to specific combinations of elements. Furthermore, most of the combinations have solid-solution phases in limited regions of composition and temperature. Thus, alloys often undergo phase separation from the high-temperature solid-solution state when the temperature is reduced. Even in such cases, we can obtain solid-solution phases at room temperature as a metastable state using a quenching technique from the high-temperature solid-solution phase. However, in certain cases, the constituent elements are immiscible, even in a high-temperature liquid phase. In those cases, solid-solution phases have not yet been obtained, because the quenching technique is not applicable to the phase-separated liquid phase.

Rh, Pd, and Ag are neighboring noble metals in the 4d transition-metal series. Each is well known as an effective catalyst for various chemical reactions.[2] If these metals could be mixed in a desired ratio, then their chemical and physical properties could be enhanced. In the Ag−Pd solid-solution system that has complete solid solubility, the hydrogen permeability is most enhanced when the ratio is Ag:Pd = 24:76. The thin film resulting from this system is used as a hydrogen-permeable membrane.[3] However, in the other two combinations, namely Pd−Rh and Ag−Rh, phase separation occurs, with complete insolubility at room temperature.[4,5] In the case of Ag−Rh, even in the liquid phase at around 2000 °C, Ag and Rh do not mix, and segregated clusters of each element form. Considering the band-filling effect in the III−V semiconductors,[6] the $Ag_{50}Rh_{50}$ solid-solution alloy is expected to have an electronic structure similar to that of Pd and to resemble Pd in terms of chemical and physical properties, since Pd is located between Rh and Ag in the periodic table. For example, one of the well-known unique properties of Pd is its ability to store hydrogen, which is attributed to its electronic structure;[7] Rh and Ag have no hydrogen-storage ability. Does the $Ag_{50}Rh_{50}$ solid-solution alloy actually absorb hydrogen? In this paper, we report the first example of a Ag−Rh solid-solution alloy exhibiting a hydrogen-storage property.

Recently, several techniques for stabilizing nonequilibrium phases at ordinary temperatures and pressures have been attracting attention. Reducing the particle size to the nanometer scale appears to be a particularly efficient technique. For example, various nonequilibrium solid-solution alloys such as Au−Pt, Au−Ni, Au−Fe, and Ag−Pt, which exist in solid solution at high temperatures or in the liquid phase, have been easily obtained as metal nanoparticles by solution chemistry methods.[8−12] This may allow the isolation of novel solid-solution alloys, even in the entirely immiscible Ag−Rh system.

Poly(*N*-vinyl-2-pyrrolidone) (PVP)-protected Ag−Rh nanoparticles were prepared by a chemical reduction method. For the 50:50 Ag−Rh nanoparticles, $AgNO_3$ and $Rh(CH_3COO)_3$ were dissolved in water in a 50:50 molar ratio. The solution was then added to ethylene glycol containing PVP at 170 °C. After cooling to room temperature, the nanoparticles were separated using a centrifuge. For other compositions, similar procedures were adopted, with appropriate stoichiometric mixtures of starting materials.

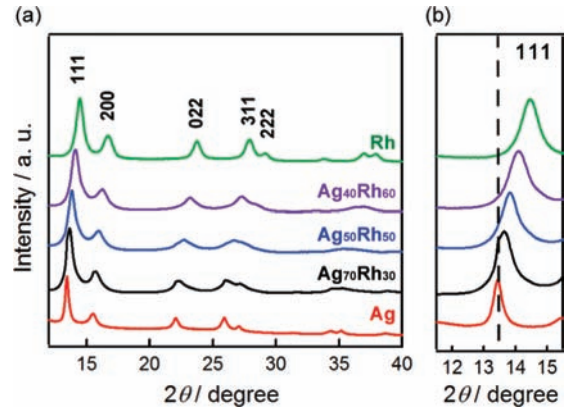

Figure 1. (a) Synchrotron X-ray powder diffraction patterns ($2\theta = 12-40°$) of Ag, Rh, and Ag−Rh nanoparticles at 303 K; (b) close-up of the $2\theta = 11-16°$ region.

Transmission electron microscope (TEM) images of the synthesized $Ag_{50}Rh_{50}$ nanoparticles were recorded on a JEOL JEM-

[†] Graduate School of Science, Kyoto University.
[#] Hokkaido University.
[‡] iCeMS, Kyoto University.
[§] JST CREST.
[⊥] Osaka Prefecture University.

10.1021/ja107362z

2000EX TEM instrument (Supporting Information, Figure S1). The size distribution was narrow, and the mean diameter was estimated to be 12.2 ± 1.6 nm by averaging over at least 300 particles.

The crystal structures of Ag_xRh_{100-x} bimetallic nanoparticles were investigated by synchrotron X-ray (λ = 0.55277 Å) powder diffraction at the beam line BL02B2, SPring-8. The diffraction patterns of the samples sealed in glass capillaries under vacuum were measured at 303 K. Figure 1 shows the X-ray diffraction (XRD) patterns of Ag and Rh and three combinations of Ag−Rh nanoparticles ($Ag_{70}Rh_{30}$, $Ag_{50}Rh_{50}$, and $Ag_{40}Rh_{60}$). All the Ag−Rh samples showed diffraction patterns consistent with single face-centered-cubic structure without signals from pure Ag or Rh phases (Figure 1a). The diffraction peaks of Ag−Rh nanoparticles shifted continuously to the higher-angle side with increasing Rh content in the Ag−Rh nanoparticles, which is in agreement with the shrinkage of the lattice parameter due to the smaller unit cell parameter of Rh (Figure 1b). This result strongly supports the formation of the atomic-level Ag−Rh alloy.

To investigate the composition of Ag and Rh atoms in the nanoparticles, elemental analyses were carried out using atomic absorption spectrophotometry (AAS) and energy-dispersive X-ray (EDX) techniques. The average stoichiometry from the AAS data was Ag:Rh = 0.51:0.49, and that from the EDX data was Ag:Rh = 0.49:0.51. Figure 2 shows elemental mapping data for a group of prepared $Ag_{50}Rh_{50}$ nanoparticles. Figure 2a shows a high-angle annular dark-field STEM (HAADF-STEM) image. Figure 2b,c shows the corresponding Ag-L and Rh-L STEM-EDX maps, respectively. Figure 2d presents an overlay map of the Ag and Rh chemical distribution. The mapping data (Figure 2d) provide visually apparent evidence of the formation of Ag−Rh solid solutions.

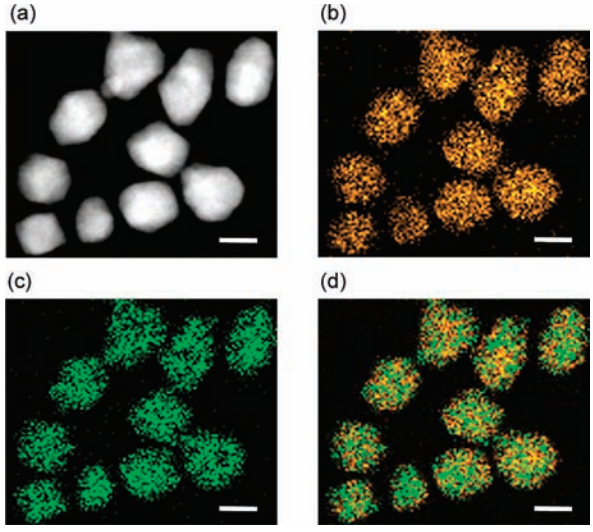

Figure 2. (a) HAADF-STEM image, (b) Ag-L STEM-EDX map, and (c) Rh-L STEM-EDX map obtained from a group of prepared $Ag_{50}Rh_{50}$ nanoparticles. (d) Reconstructed overlay image of the maps shown in panels b and c (green, Rh; orange, Ag). The scale bars correspond to 10 nm.

We further characterized the Ag−Rh nanoparticles by EDX line scanning analysis (Supporting Information, Figure S2). The line-scan position of the nanoparticle is denoted by the white line in the inset of Figure S2. The compositional line profiles of Ag and Rh on a $Ag_{50}Rh_{50}$ nanoparticle show that atomic-level Ag−Rh alloying successfully occurs.

To investigate the hydrogen-storage properties of the Ag−Rh nanoparticles, we measured hydrogen pressure−composition isotherms. Studies on hydrogen-storage properties give important information related to the electronic state of metals.[13] As shown in Figure 3a, the total amount of hydrogen absorption of $Ag_{50}Rh_{50}$ nanoparticles was 0.09 H/M (M = $Ag_{0.5}Rh_{0.5}$) at ca. 100 kPa, whereas the absorptions of $Ag_{70}Rh_{30}$ and $Ag_{40}Rh_{60}$ nanoparticles were 0.05 H/M (M = $Ag_{0.7}Rh_{0.3}$) and 0.06 H/M (M = $Ag_{0.4}Rh_{0.6}$), respectively. The total amount of hydrogen absorption reached a maximum at the ratio of Ag:Rh = 50:50, where the electronic structure is expected to be similar to that of Pd. As can be seen in Figure 3a, the amount of hydrogen absorption depends on the metal composition of the alloy. Accordingly, this difference in the amounts of hydrogen absorption implies a difference in the electronic structures of Ag_xRh_{100-x} nanoparticles.

Solid-state ^2H NMR measurements were performed to investigate the state of ^2H in the Ag−Rh nanoparticles (Figure 3b-2). In the spectrum of $Ag_{50}Rh_{50}$ nanoparticles, a broad absorption line at ca. −2.3 ppm, with a full width at half-maximum of ca. 146 ppm, and a sharp line around 0 ppm were observed. In the spectrum of $^2H_2$ gas (Figure 3b-4), only a sharp line at 3.4 ppm was obtained. On comparison of these spectra, it is reasonable to attribute the sharp line in the spectrum of the $Ag_{50}Rh_{50}$ particle to free deuterium gas ($^2H_2$) and the broad component to absorbed deuterium atoms (^2H) in the particles. The broad absorption lines of deuterium absorbed inside the lattices of $Ag_{70}Rh_{30}$ and $Ag_{40}Rh_{60}$ nanoparticles were observed at ca. 4.4 and −132.9 ppm, respectively (Figure 3b-1,3). These chemical shifts that give rise to the broad absorption lines suggest that the deuterium atoms inside the nanoparticles perceive the different potentials, and atomic-level alloying occurs in the Ag−Rh system.

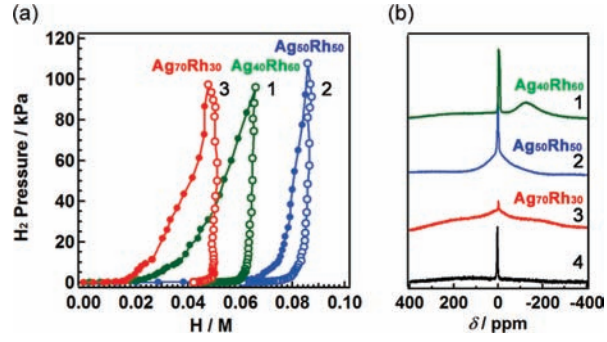

Figure 3. (a) Pressure−composition isotherms of (1) $Ag_{40}Rh_{60}$, (2) $Ag_{50}Rh_{50}$, and (3) $Ag_{70}Rh_{30}$ nanoparticles (●, absorption at 303 K; ○, desorption at 303 K). (b) Solid-state ^2H NMR spectra for (1) $Ag_{40}Rh_{60}$, (2) $Ag_{50}Rh_{50}$, and (3) $Ag_{70}Rh_{30}$ nanoparticles and (4) $^2H_2$ gas. All the samples were measured under 86.7 kPa of $^2H_2$ gas at 303 K.

In summary, we have used the chemical reduction method to obtain, for the first time, solid solutions of PVP-protected Ag−Rh alloys that are intimately mixed at the atomic level. The atomic-level Ag−Rh alloying was confirmed by means of EDX and XRD measurements. It is known that Ag and Rh do not mix but form segregated clusters of each element, even in the liquid phase around 2000 °C.[4] Consequently, solid-solution Ag−Rh alloys cannot be obtained, even by means of quenching techniques, and no knowledge of the structure or the electronic structure of the alloys was available. Our results contribute to the limited knowledge in this area. Furthermore, the prepared Ag−Rh alloys show hydrogen-storage properties; the $Ag_{50}Rh_{50}$ alloy exhibits the highest level of hydrogen absorption in the alloys. However, the H/M value of $Ag_{50}Rh_{50}$ is about half that of a bulk Pd. From our experimental results, we conclude that the $Ag_{50}Rh_{50}$ solid-solution alloy has an electronic structure similar to that of Pd (that is to say, "modern

alchemy"). Following on from the discovery of the Ag−Rh solid-solution alloy, we envisage the development of new solid-solution alloys of immiscible Ag−Ni, Au−Rh, Cu−Ru, and others that exhibit phase-segregated structures, even in the high-temperature liquid phase.[5,14,15]

Acknowledgment. This work was partly supported by Grants-in-Aid for the Global COE Program, "Science for Future Molecular Systems", and Elements Science and Technology Project from the MEXT, Japan, and Research Fellowships for Young Scientists No. 22·3504 from the JSPS.

Supporting Information Available: Experimental details, particle compositions, TEM images, line scanning of $Ag_{50}Rh_{50}$ nanoparticles, UV−Vis spectra, and XPS spectra. This material is available free of charge via the Internet at http://pubs.acs.org

References

(1) (a) Turchi, P. E. A.; Drchal, V.; Kudrnovský, J. *Phys. Rev. B* **2006**, *74*, 064202-1-12. (b) Mena, F. P.; DiTusa, J. F.; van der Marel, D.; Aeppli, G.; Young, D. P.; Damascelli, A.; Mydosh, J. A. *Phys. Rev. B* **2006**, *73*, 085205-1-7. (c) Eagleton, T. S.; Mallet, J.; Cheng, X.; Wang, J.; Chien, C.; Searson, P. C. *J. Electrochem. Soc.* **2005**, *152*, C27–C31.
(2) (a) Bowker, M. *Chem. Soc. Rev.* **2008**, *37*, 2204–2211. (b) Inderwildi, O. R.; Jenkins, S. J.; King, D. A. *J. Am. Chem. Soc.* **2008**, *130*, 2213–2220. (c) Guo, J.; Hsu, A.; Chu, D.; Chen, R. *J. Phys. Chem. C* **2010**, *114*, 4324–4330. (d) Cobley, C. M.; Campbell, D. J.; Xia, Y. *Adv. Mater.* **2008**, *20*, 748–752.
(3) Holleck, G. L. *J. Phys. Chem.* **1970**, *74*, 503–511.
(4) Zarkevich, N. A.; Tan, T. L.; Johnson, D. D. *Phys. Rev. B* **2007**, *75*, 104203−1-12.
(5) Massalski, T. B.; Okamoto, H.; Subramanian, P. R.; Kacprzak, L. *Binary Alloy Phase Diagrams*; ASM International: Materials Park, OH, 1996.
(6) Gera, V. B.; Gupta, R.; Jain, K. P. *J. Phys.: Condens. Matter* **1989**, *1*, 4913–4930.
(7) (a) Papaconstantopoulos, D. A.; Klein, B. M.; Economou, E. N.; Boyer, L. L. *Phys. Rev. B* **1978**, *17*, 141–150. (b) Fazle Kibria, A. K. M.; Sakamoto, Y. *Int. J. Hydrogen Energy* **2000**, *25*, 853–859. (c) Vuillemin, J. J.; Priestly, M. G. *Phys. Rev. Lett.* **1965**, *14*, 307–309. (d) Wicke, E. *J. Less-Common Met.* **1984**, *101*, 17–33.
(8) (a) Zou, S.; Jackson, G. S.; Eichhorn, B. *Adv. Funct. Mater.* **2007**, *17*, 3099–3104. (b) Hernández-Fernández, P.; Rojas, S.; Ocón, P.; Gómez de la Fuente, J. L.; San Fabián, J.; Sanza, J.; Peña, M. A.; García-García, F. J.; Terreros, P.; Fierro, J. L. G. *J. Phys. Chem. C* **2007**, *111*, 2913–2923. (c) Lang, H.; Maldonado, S.; Stevenson, K. J.; Chandler, B. D. *J. Am. Chem. Soc.* **2004**, *126*, 12949–12956.
(9) Chiang, I.; Chen, Y.; Chen, D. *J. Alloys Compd.* **2009**, *468*, 237–245.
(10) Lu, D.; Domen, K.; Tanaka, K. *Langmuir* **2002**, *18*, 3226–3232.
(11) (a) Chiang, I.; Chen, D. *Adv. Funct. Mater.* **2007**, *17*, 1311–1316. (b) Dahal, N.; Chikan, V.; Jasinski, J.; Leppert, V. J. *Chem. Mater.* **2008**, *20*, 6389–6395.
(12) Torigoe, K.; Nakajima, Y.; Esumi, K. *J. Phys. Chem.* **1993**, *97*, 8304–8309.
(13) (a) Kobayashi, H.; Yamauchi, M.; Ikeda, R.; Kitagawa, H. *Chem. Commun.* **2009**, *32*, 4806–4808. (b) Kobayashi, H.; Yamauchi, M.; Kitagawa, H.; Kubota, Y.; Kato, K.; Takata, M. *J. Am. Chem. Soc.* **2008**, *130*, 1818–1819. (c) Kobayashi, H.; Yamauchi, M.; Kitagawa, H.; Kubota, Y.; Kato, K.; Takata, M. *J. Am. Chem. Soc.* **2008**, *130*, 1828–1829. (d) Yamauchi, M.; Ikeda, R.; Kitagawa, H.; Takata, M. *J. Phys. Chem. C* **2008**, *112*, 3294–3299. (e) Yamauchi, M.; Kobayashi, H.; Kitagawa, H. *ChemPhysChem* **2009**, *10*, 2566–2576. (f) Kobayashi, H.; Yamauchi, M.; Kitagawa, H.; Kubota, Y.; Kato, K.; Takata, M. *J. Am. Chem. Soc.* **2010**, *132*, 5576–5577.
(14) Liu, X. J.; Gao, F.; Wang, C. P.; Ishida, K. *J. Electron. Mater.* **2008**, *37*, 210–217.
(15) Raevskaya, M. V.; Yanson, I. E.; Tatarkina, A. L.; Sokolova, I. G. *J. Less-Common Met.* **1987**, *132*, 237–241.

JA107362Z